



**HAL**  
open science

# Analytical Port Inversion For A Flexible Model In The Two-Input Two-Output Port Approach

Antonio Finozzi, Francesco Sanfedino, Daniel Alazard

► **To cite this version:**

Antonio Finozzi, Francesco Sanfedino, Daniel Alazard. Analytical Port Inversion For A Flexible Model In The Two-Input Two-Output Port Approach. 10th ECCOMAS Thematic Conference on MULTIBODY DYNAMICS, Dec 2021, Budapest, Hungary. pp.159-170. hal-03533909

**HAL Id: hal-03533909**

**<https://hal.science/hal-03533909>**

Submitted on 19 Jan 2022

**HAL** is a multi-disciplinary open access archive for the deposit and dissemination of scientific research documents, whether they are published or not. The documents may come from teaching and research institutions in France or abroad, or from public or private research centers.

L'archive ouverte pluridisciplinaire **HAL**, est destinée au dépôt et à la diffusion de documents scientifiques de niveau recherche, publiés ou non, émanant des établissements d'enseignement et de recherche français ou étrangers, des laboratoires publics ou privés.



## Open Archive Toulouse Archive Ouverte

OATAO is an open access repository that collects the work of Toulouse researchers and makes it freely available over the web where possible

This is an author's version published in: <http://oatao.univ-toulouse.fr/28762>

### Official URL:

[https://eccomasmultibody2021.mm.bme.hu/Files/EccomasMultybody2021\\_Proceedings.pdf](https://eccomasmultibody2021.mm.bme.hu/Files/EccomasMultybody2021_Proceedings.pdf)

### To cite this version:

Finozzi, Antonio and Sanfedino, Francesco  and Alazard, Daniel  *Analytical Port Inversion For A Flexible Model In The Two-Input Two-Output Port Approach*. (2021) In: 10th ECCOMAS Thematic Conference on MULTIBODY DYNAMICS, 12 December 2021 - 15 December 2021 (Budapest, Hungary).

Any correspondence concerning this service should be sent to the repository administrator: [tech-oatao@listes-diff.inp-toulouse.fr](mailto:tech-oatao@listes-diff.inp-toulouse.fr)

# Analytical Port Inversion For A Flexible Model In The Two-Input Two-Output Port Approach

A. Finozzi<sup>1</sup>, F. Sanfedino<sup>1</sup>, D. Alazard<sup>1</sup>

<sup>1</sup> Institut Supérieur de l'Aéronautique  
et de l'Espace (ISAE-SUPAERO)  
Université de Toulouse  
31055 Toulouse, FRANCE

[antonio.finozzi, daniel.alazard, francesco.sanfedino]@isae-supaeo.fr

## ABSTRACT

In the context of multi-body modeling techniques, this paper introduces a new analytical approach to build a Two-Input-Two-Output Port (TITOP) model for a *clamped-clamped* flexible appendage. By expanding the previous work found in literature, which relied on numerical procedures, this model represents a fundamental block for the construction of parametric multi-body systems in a sub-structuring approach, such as closed-loop kinematic mechanisms. Specifically, this new procedure allows to assemble a linear state-space system by analytically inverting the input-output channels of the original *clamped-free* TITOP model. This analytical method presents the advantage of avoiding non-physical behaviors introduced by numerical inversions as well as removing the need to reduce the quasi-zero poles associated with the non-analytical model. This paper presents the mathematical formulation of the system, as well as the formalism behind the method, and an illustrative case study to showcase the advantages of this approach.

**Keywords:** Multibody dynamics, Analytical Inversion, Linear System, Closed-Loop Kinematics.

## 1 INTRODUCTION

In the past decades, structural and control co-design has attracted a lot of attention due to its ability of merging multiple multidisciplinary requirements in a single design flow. Moreover, the increasing use of large structures and appendages for Space applications has rendered flexible modal analysis mandatory for the design of proper spacecraft control laws.

In order to tackle the non-trivial modeling and analysis of these large and complex space systems, a sub-structuring technique using a multi-body approach is often considered to conceptually simplify the model. Seeing the overall structure as an assembly of multiple simpler sub-systems with increasing complexity has also the advantage of handling different types of boundary conditions at block assemblage level and easy sub-system validation.

The wide use of this approach for space applications has raised a significant interest in the development of proper modeling techniques that can prove to be versatile enough to account for multiple multi-body configurations, ranging from open-loop chains to closed-loops mechanisms.

Many sub-structuring techniques can be found in literature. A common approach relies on approximations linked to the Finite Element Method (FEM) or the Assumed Modes Method (AMM) [1]. However, these methods are heavily influenced by the set of predetermined boundary conditions assigned to the model, which may be drastically variable,

for example by time-varying mass changes in the system. Another approach often used is the Transfer Matrix Method (TMM) [2], which creates a transfer matrix that links up the state vectors (generalized accelerations and forces) of the two extremities of the flexible body. This has also been linked with the Finite Element Method in order to reduce computational times in solving the eigenvalue problem (FE-TMM). These methods are particularly well suited for serially connected bodies and open-chain structures. Their major drawback is the inversion problems of the model, whose matrices may be non-square or non-invertible depending on the boundary conditions. Moreover, these approaches are not optimal for a multi-body tree-like structures, where multiple appendages are connected to a single central parent body: in this case the interest is finding the dynamic relation between state vectors in the same root point for each sub-structure. Methods based on effective mass/inertia of the appendages [3] represent a viable option to solve this last problem, but they lose the complete vibrational behavior description, as they aim at delivering only the dynamic relation of state variable at the appendage root point with a simplified model of the body.

The Two-Input-Two-Output Port (TITOP) Model, a direct dynamic approach initially proposed in [4], overcomes these issues. The structure is conceived as a minimal state-space transfer between the accelerations and wrenches at the extremity points of the appendage and embeds both the direct and inverse dynamics: the IN/OUT channels are easily numerically invertible to account for multiple boundary conditions. Moreover, as seen in [5], this approach in a block-diagram model permits the design of closed-chain multi-body systems for any boundary conditions by creating feedback loops and inverting IN/OUT channels. These models, already implemented in a toolbox developed at ISAE-Supaero - the Satellite Dynamics Toolbox (SDT) [6]- represent the basis of this research.

Nevertheless, the application of the numerical channel inversion proposed in [5] shows some critical aspects, specifically in obtaining the *clamped-clamped* boundary conditions. For this boundary condition configuration twelve rigid modes are expected to be at exactly zero frequency. However, because of numerical issues in the channel inversion, these modes present a quasi-null value instead. This issue, which may seem trivial at single beam level, can have a huge impact in the context of sub-structuring models: it may introduce numerical issues due to block repetitions as well as increasing the effort for model reduction at global structure level.

This research therefore proposes a new approach to obtain a TITOP *clamped-clamped* model, introducing a novel analytical procedure to invert the TITOP channels to obtain a model which does not present the previously discussed numerical issues. This was achieved by relying on a modal transformation of the state variables, distinguishing from flexible and junction modes, as introduced in [3] and later on applied by [7].

In the first section, the general formalism used to define flexible and junction modes is detailed, as well as how these concepts were applied to the formulation of the TITOP model. This will outline the basis for the mathematical formulation of the analytically inverted TITOP model presented in section 3. A simple example finally proves the increased accuracy of the proposed framework.

## 2 ANALYTICAL BEAM MODEL

### 2.1 Formalism Adopted

Let us consider a generic flexible appendage. A common approach used to characterize its vibrational response is to use modal analysis to find normal modes whose superposition describes the flexible behavior of the body.

The formalism adopted in this paper slightly varies from this classic approach. The vector of Degrees of Freedom (DOFs)  $\mathbf{u}$  is divided into two sub-vectors, using the formalism proposed in [3]: internal DOFs  $\mathbf{u}_i$  and junction DOFs  $\mathbf{u}_j$ . The latter are generally associated to boundary conditions or interfaces with other bodies. They are mostly reserved for parts of the structure where a generic imposed motion is applied. While the internal DOFs respond with a motion  $\mathbf{u}_i, \dot{\mathbf{u}}_i, \ddot{\mathbf{u}}_i$  to a force/torque forcing term  $\mathbf{F}_i$ , the junction DOFs respond with a reaction force/torque  $\mathbf{F}_j$  to an imposed motion-type excitation  $\mathbf{u}_j, \dot{\mathbf{u}}_j, \ddot{\mathbf{u}}_j$ . The equations of motion for a dynamic system may be written according to the following subdivision of the DOFs:

$$\begin{bmatrix} \mathbf{M}_{ii} & \mathbf{M}_{ij} \\ \mathbf{M}_{ij}^T & \mathbf{M}_{jj} \end{bmatrix} \begin{bmatrix} \ddot{\mathbf{u}}_i \\ \ddot{\mathbf{u}}_j \end{bmatrix} + \begin{bmatrix} \mathbf{C}_{ii} & \mathbf{C}_{ij} \\ \mathbf{C}_{ij}^T & \mathbf{C}_{jj} \end{bmatrix} \begin{bmatrix} \dot{\mathbf{u}}_i \\ \dot{\mathbf{u}}_j \end{bmatrix} + \begin{bmatrix} \mathbf{K}_{ii} & \mathbf{K}_{ij} \\ \mathbf{K}_{ij}^T & \mathbf{K}_{jj} \end{bmatrix} \begin{bmatrix} \mathbf{u}_i \\ \mathbf{u}_j \end{bmatrix} = \begin{bmatrix} \mathbf{F}_i \\ \mathbf{F}_j \end{bmatrix} \quad (1)$$

where we can identify the three fundamental symmetrical matrices: the mass matrix  $\mathbf{M}$ , the damping matrix  $\mathbf{C}$  and the stiffness matrix  $\mathbf{K}$ , each one composed of sub-matrices associated with both types of DOFs (internal and junction). The modes are obtained by analyzing the homogeneous undamped harmonic equations of motion. To obtain the homogeneous system, the forcing terms  $\mathbf{F}_i$  and  $\mathbf{u}_j$  are suppressed from the previous equation. Additionally, the undamped equations are considered by setting the whole damping matrix  $\mathbf{C} = \mathbf{0}$ . This approach leads to two sets of equations: the first one allows for the definition of the normal modes.

$$\mathbf{M}_{ii}\ddot{\mathbf{u}}_i + \mathbf{K}_{ii}\mathbf{u}_i = \mathbf{0} \quad (2)$$

The normal modes of the system, denoted with  $\Phi_{ik}$ , can be derived by imposing the harmonic solution  $\mathbf{u}_i = \mathbf{U}_i e^{j\omega t}$ :

$$(-\omega^2 \mathbf{M}_{ii} + \mathbf{K}_{ii})\mathbf{U}_i = \mathbf{0} \quad (3)$$

By solution of the corresponding eigenvalue problem, the eigenvalues  $\omega_k$  are obtained, as well as the normal eigenmodes  $\Phi_{ik}$  where  $k$  denotes the association with the  $k$ -eigenvalue frequency  $f_k = \frac{\omega_k}{2\pi}$ . These modes have diagonalizing properties on both  $\mathbf{M}_{ii}$  and  $\mathbf{K}_{ii}$ .

Furthermore, it is possible to define static modes denoted as junction modes  $\Psi$  by imposing a unit displacement  $\mathbf{u}_j = 1$  on the second homogeneous undamped equation derived from Eq. 1. These modes verify:

$$\begin{aligned} \Psi_{jj} &= \mathbf{I}_{jj}, & \mathbf{K}_{ii}\Psi_{ij} + \mathbf{K}_{ij} &= \mathbf{0} \\ \implies \Psi_{ij} &= -\mathbf{K}_{ii}^{-1}\mathbf{K}_{ij} \end{aligned} \quad (4)$$

An important remark is that the static modes can be interpreted as static transmissibility in displacements between the DOFs  $i$  and  $j$ . The two sets of modes can be exploited to perform a modal superposition in order to describe the displacement vector  $\mathbf{u} = [\mathbf{u}_i, \mathbf{u}_j]^T$  as described as follows:

$$\begin{bmatrix} \mathbf{u}_i \\ \mathbf{u}_j \end{bmatrix} = \begin{bmatrix} \Phi_{ik} & \Psi_{ij} \\ \mathbf{0} & \mathbf{I}_{jj} \end{bmatrix} \begin{bmatrix} \boldsymbol{\eta}_k \\ \mathbf{u}_j \end{bmatrix} \quad (5)$$

The first row expresses the absolute displacement  $\mathbf{u}_i$  as composed by an interpolation of internal relative DOFs, given by modal coordinates  $\boldsymbol{\eta}_k$ , and junction displacements  $\mathbf{u}_j$ . The second row states that the junction displacements are conserved. By performing this superposition, a new set of equations of motion can be derived from Eq. 1:

$$\begin{bmatrix} \mathbf{m}_{kk} & \mathbf{L}_{kj} \\ \mathbf{L}_{kj}^T & \overline{\mathbf{M}}_{jj} \end{bmatrix} \begin{bmatrix} \dot{\boldsymbol{\eta}}_k \\ \dot{\mathbf{u}}_j \end{bmatrix} + \begin{bmatrix} \mathbf{c}_{kk} & \mathbf{0}_{jk}^T \\ \mathbf{0}_{jk} & \mathbf{0}_{jj} \end{bmatrix} \begin{bmatrix} \boldsymbol{\eta}_k \\ \mathbf{u}_j \end{bmatrix} + \begin{bmatrix} \mathbf{k}_{kk} & \mathbf{0}_{jk}^T \\ \mathbf{0}_{jk} & \overline{\mathbf{K}}_{jj} \end{bmatrix} \begin{bmatrix} \boldsymbol{\eta}_k \\ \mathbf{u}_j \end{bmatrix} = \begin{bmatrix} \boldsymbol{\Phi}_{ik}^T \mathbf{F}_i \\ \boldsymbol{\Psi}_{ij}^T \mathbf{F}_i + \mathbf{F}_j \end{bmatrix} \quad (6)$$

Where:

- $\mathbf{m}_{kk} = \boldsymbol{\Phi}_{ik}^T \mathbf{M}_{ii} \boldsymbol{\Phi}_{ik}$ : diagonal matrix of generalized masses  $m_k$ . By selecting a normalized set of  $\boldsymbol{\Phi}_{ik}$ , it corresponds to the identity matrix  $\mathbf{I}_{kk}$ ;
- $\mathbf{c}_{kk} = \boldsymbol{\Phi}_{ik}^T \mathbf{C}_{ii} \boldsymbol{\Phi}_{ik}$ : matrix of generalized damping. *A priori* this matrix is fully populated but under hypothesis of proportional damping w.r.t mass and stiffness or lightly damped structure the matrix can be considered diagonal with  $\mathbf{c}_{kk} = \text{diag}(2\omega_k \xi m_k)$ , where  $\xi$  is the damping coefficient for the appendix;
- $\mathbf{k}_{kk} = \boldsymbol{\Phi}_{ik}^T \mathbf{K}_{ii} \boldsymbol{\Phi}_{ik}$ : diagonal mass of generalized stiffness  $k_k = m_k \omega_k^2$ ;
- $\mathbf{L}_{kj} = \boldsymbol{\Phi}_{ik}^T [\mathbf{M}_{ii} \mathbf{M}_{ij}] \begin{bmatrix} \boldsymbol{\Psi}_{ij} \\ \mathbf{I}_{jj} \end{bmatrix} = \boldsymbol{\Phi}_{ik}^T (\mathbf{M}_{ii} \boldsymbol{\Psi}_{ij} + \mathbf{M}_{ij})$ : matrix of participation factors. It expresses the coupling between the normal and junction modes.
- $\overline{\mathbf{M}}_{jj} = \boldsymbol{\Psi}_{ij}^T \mathbf{M}_{ii} \boldsymbol{\Psi}_{ij} + \boldsymbol{\Psi}_{ij}^T \mathbf{M}_{ij} + \mathbf{M}_{ij}^T \boldsymbol{\Psi}_{ij} + \mathbf{M}_{jj}$ : condensed mass matrix. In the case of a rigid statically determined junction  $j = r$ , it is equal to structure rigid body mass matrix which includes its properties on mass, center of mass and inertia relative to the unique node reference frame.
- $\overline{\mathbf{K}}_{jj} = \mathbf{K}_{jj} - \mathbf{K}_{ij}^T \mathbf{K}_{ii} \mathbf{K}_{ij}$ : condensed stiffness matrix. In the case of a rigid statically determined junction, it is equal to zero.

The formalism introduced here has been applied directly to TITOP models to perform modal analysis in [7]. In the following section the same procedure will be applied specifically for the TITOP beam model and it will provide the fundamental basics for the analytical inversion described in section 3.

## 2.2 Application to TITOP Model

### 2.2.1 TITOP Model Presentation

Let us consider a uniform flexible appendage  $\mathcal{L}_i$  as in Fig. 1, defined by means of two points: point  $P$ , the point to which the flexible appendage is linked to a parent structure  $\mathcal{L}_{i-1}$ , and point  $C$ , where a child body  $\mathcal{L}_{i+1}$  is linked to the beam.

In the beam model of the appendage  $\mathcal{L}_i$ , *clamped-free* boundary conditions are considered: the joint at point  $P$  is considered rigid and statically determinate, with the parent body  $\mathcal{L}_{i-1}$  imposing a motion on  $\mathcal{L}_i$ , while point  $C$  is internal and unconstrained and the action of  $\mathcal{L}_{i+1}$  is by mean of a transmitted effort. This can be done without any loss of generality as seen in [5].

The flexible appendix is modeled using a beam model, taken from [6], which describes the 3D vibrational behavior of  $\mathcal{L}_i$  by considering its bending in planes  $(x, z)$  and  $(x, y)$ , torsion around the  $x$ -axis and traction along the  $x$ -axis in the local frame  $\mathcal{R}_0$ . The resulting TITOP model  $\mathbf{D}_{PC}^{\mathcal{L}_i}(s)$ , displayed in Fig. 1, is a  $\{12 \times 12\}$  linear dynamic model function of the Laplace variable  $s$ . Its inputs are:

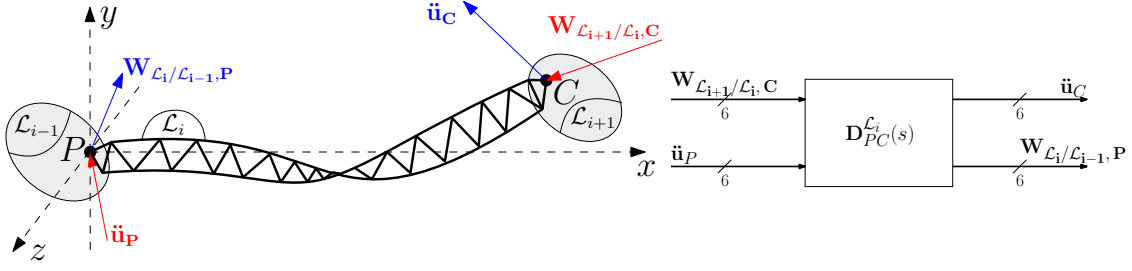


**Figure 1.** TITOP model and nomenclature for a generic flexible appendage  $\mathcal{L}_i$

- $\mathbf{W}_{\mathcal{L}_{i+1}/\mathcal{L}_i,C}$ : The  $\{6 \times 1\}$  Wrench (Forces and Torques) exerted by the body  $\mathcal{L}_{i+1}$  to  $\mathcal{L}_i$  at point C;
- $\ddot{\mathbf{u}}_P$ : The  $\{6 \times 1\}$  accelerations (linear and angular) imposed by the parent body  $\mathcal{L}_{i-1}$  at point P to  $\mathcal{L}_i$ ;

while the outputs are:

- $\ddot{\mathbf{u}}_C$ : The  $\{6 \times 1\}$  components of the accelerations of point C;
- $\mathbf{W}_{\mathcal{L}_i/\mathcal{L}_{i-1},P}$ : The  $\{6 \times 1\}$  Wrench (Forces and Torques) transferred by  $\mathcal{L}_i$  to the parent structure  $\mathcal{L}_{i-1}$  at point P.

### 2.2.2 Mathematical Formulation

The vector of DOFs used in the description of the vibrational behaviors is assembled in order to contain two distinct entities: the kinematic parameters of point P and the relative deformation at point C with respect to point P. The beam is defined by the main direction of vector  $\overline{PC}$ , which defines the x-axis of the local frame of reference. This mathematical formulation stems from the one proposed in [5], where a full description of the DOFs and the corresponding structural matrices can be found.

For the two bending models, the first 4 modes are considered and the DOFs adopted are reported in Eq. 7 and Eq. 8.

$$\tilde{\mathbf{q}} = \left[ y_P, \Phi_P^z, \frac{T_{bP}^z}{EI_z}, y_C - l\Phi_P^z - y_P, \Phi_C^z - \Phi_P^z, \frac{T_{bC}^z}{EI_z} \right]^T \quad (7)$$

$$\tilde{\mathbf{p}} = \left[ z_P, \Phi_P^y, \frac{T_{bP}^y}{EI_y}, z_C - l\Phi_P^y - z_P, \Phi_C^y - \Phi_P^y, \frac{T_{bC}^y}{EI_y} \right]^T \quad (8)$$

Here we denote with  $(y_P, z_P)$  and  $(y_C, z_C)$  the displacement components of  $\mathbf{u}_P$  and  $\mathbf{u}_C$  along the corresponding axis. In the same manner,  $(\Phi_P^z, \Phi_P^y)$  and  $(\Phi_C^z, \Phi_C^y)$  are the angular slopes of the deflection on the indicated axis. Finally,  $(T_{b,C}^y, T_{b,C}^z)$  and  $(T_{b,P}^y, T_{b,P}^z)$  are the bending moments at the two endpoints.

By means of the DOFs introduced in Eq. 7 and Eq. 8, both mass and stiffness matrices may be derived, which are denoted with  $\tilde{\mathbf{M}}_y, \tilde{\mathbf{K}}_y$  for  $(x, y)$  bending and  $\tilde{\mathbf{M}}_z, \tilde{\mathbf{K}}_z$  for  $(x, z)$  bending.

The same approach may be applied for torsion and axial deformations, by taking into account the DOFs vector of Eq. 9-10, originally proposed by [5]:

$$\tilde{\boldsymbol{\theta}} = \left[ \theta_P, \theta_C - \theta_P \right]^T = \left[ \theta_P, \delta_\theta \right]^T \quad (9)$$

$$\tilde{\mathbf{u}}_x = \left[ x_P, x_C - x_P \right]^T = \left[ x_P, \delta_u \right]^T \quad (10)$$

In this case only their fundamental mode is taken into account. From these vectors the mass and stiffness matrices  $\tilde{\mathbf{M}}_\theta$ ,  $\tilde{\mathbf{K}}_\theta$  and  $\tilde{\mathbf{M}}_u$ ,  $\tilde{\mathbf{K}}_u$  are obtained.

In order to obtain the *global* mass and stiffness matrices ( $\tilde{\mathbf{M}}_{gl}$ ,  $\tilde{\mathbf{K}}_{gl}$ ) for the whole beam, the sub-matrices corresponding to each vibrational behavior may be assembled in a block diagonal fashion, so that it corresponds to the global DOFs vector  $\tilde{\mathbf{d}}_{gl}$ .

$$\tilde{\mathbf{d}}_{gl} = [\tilde{\mathbf{q}}, \tilde{\mathbf{p}}, \tilde{\boldsymbol{\theta}}, \tilde{\mathbf{u}}_x]^T \quad (11)$$

$$\tilde{\mathbf{M}}_{gl} = \begin{bmatrix} \tilde{\mathbf{M}}_y & \mathbf{0} & \mathbf{0} & \mathbf{0} \\ \mathbf{0} & \tilde{\mathbf{M}}_z & \mathbf{0} & \mathbf{0} \\ \mathbf{0} & \mathbf{0} & \tilde{\mathbf{M}}_\theta & \mathbf{0} \\ \mathbf{0} & \mathbf{0} & \mathbf{0} & \tilde{\mathbf{M}}_u \end{bmatrix}, \quad \tilde{\mathbf{K}}_{gl} = \begin{bmatrix} \tilde{\mathbf{K}}_y & \mathbf{0} & \mathbf{0} & \mathbf{0} \\ \mathbf{0} & \tilde{\mathbf{K}}_z & \mathbf{0} & \mathbf{0} \\ \mathbf{0} & \mathbf{0} & \tilde{\mathbf{K}}_\theta & \mathbf{0} \\ \mathbf{0} & \mathbf{0} & \mathbf{0} & \tilde{\mathbf{K}}_u \end{bmatrix} \quad (12)$$

A permutation on these matrices can be performed in order to obtain a DOFs division as seen in Eq. 1, through the use of a permutation matrix  $\mathbf{P}$ . The resulting global mass and stiffness matrices, as well as the vector of DOFs  $\mathbf{d}_{gl}$  is shown in Eq. 13 and Eq. 14. The point  $P$  is a junction node, therefore we can substitute the subscript  $j$  with  $P$ .

$$\mathbf{d}_{gl} = [\mathbf{u}_P, \mathbf{u}_f]^T = \mathbf{P}\tilde{\mathbf{d}}_{gl} \quad (13)$$

$$\mathbf{M}_{gl} = \mathbf{P}\tilde{\mathbf{M}}_{gl}\mathbf{P}^T = \begin{bmatrix} \mathbf{M}_{rr} & \mathbf{M}_{rf} \\ \mathbf{M}_{fr} & \mathbf{M}_{ff} \end{bmatrix}, \quad \mathbf{K}_{gl} = \mathbf{P}\tilde{\mathbf{K}}_{gl}\mathbf{P}^T = \begin{bmatrix} \mathbf{0}_{rr} & \mathbf{0}_{rf} \\ \mathbf{0}_{fr} & \mathbf{K}_{ff} \end{bmatrix} \quad (14)$$

The matrix  $\mathbf{M}_{rr}$  represents the mass matrix of the *rigid* body at point  $P$ , while  $\mathbf{M}_{fr}$  and  $\mathbf{M}_{rf}$  are the coupling terms between the displacement of point  $P$  and the internal *flexible* DOFs of vector  $\mathbf{u}_f$ . The vectors  $\mathbf{u}_P$  and  $\mathbf{u}_f$  are given by:

$$\begin{aligned} \mathbf{u}_P &= [x_P, y_P, z_P, \theta_P, \Phi_P^y, \Phi_P^z]^T \\ \mathbf{u}_f &= [x_C - x_P, y_C - y_P - l\Phi_P^z, z_C - z_P - l\Phi_P^y, \theta_C - \theta_P, \\ &\quad \Phi_C^y - \Phi_P^y, \Phi_C^z - \Phi_P^z, \frac{T_{bP}^y}{EI_y}, \frac{T_{bP}^z}{EI_z}, \frac{T_{bC}^y}{EI_y}, \frac{T_{bC}^z}{EI_z}]^T \end{aligned}$$

We introduce  $\boldsymbol{\tau}_{CP}$  as the kinematic link between the internal node  $C$  and the junction node  $P$ :

$$\boldsymbol{\tau}_{CP} = \begin{bmatrix} \mathbf{I}_{3 \times 3}, * \mathbf{CP} \\ \mathbf{0}_{3 \times 3} \mathbf{I}_{3 \times 3} \end{bmatrix} \quad (15)$$

Where  $*\mathbf{CP}$  is the skew-symmetric matrix obtained from the vector from point  $C$  to point  $P$ . It can be verified that matrix  $\boldsymbol{\tau}_{CP}$  corresponds exactly to the junction modes matrix  $\boldsymbol{\Psi}_{ij}$  introduced in section 2. By performing modal analysis on this system, remarking that by imposing Eq. 4 we get  $\boldsymbol{\Psi}_{ij} = 0$ , the following expression can be found:

$$\begin{bmatrix} \mathbf{M}_{rr} & \mathbf{L}_{kP}^T \\ \mathbf{L}_{kP} & \mathbf{I}_{kk} \end{bmatrix} \begin{bmatrix} \ddot{\mathbf{u}}_P \\ \ddot{\boldsymbol{\eta}}_k \end{bmatrix} + \begin{bmatrix} \mathbf{0}_{PP} & \mathbf{0}_{kP} \\ \mathbf{0}_{kP}^T & \mathbf{c}_{kk} \end{bmatrix} \begin{bmatrix} \dot{\mathbf{u}}_P \\ \dot{\boldsymbol{\eta}}_k \end{bmatrix} + \begin{bmatrix} \mathbf{0}_{PP} & \mathbf{0}_{kP} \\ \mathbf{0}_{kP}^T & \mathbf{k}_{kk} \end{bmatrix} \begin{bmatrix} \mathbf{u}_P \\ \boldsymbol{\eta}_k \end{bmatrix} = \begin{bmatrix} \boldsymbol{\Phi}_{Ck}^T \mathbf{W}_{\mathcal{L}_{i+1}/\mathcal{L}_i, C} \\ \boldsymbol{\tau}_{CP}^T \mathbf{W}_{\mathcal{L}_{i+1}/\mathcal{L}_i, C} - \mathbf{W}_{\mathcal{L}_i/\mathcal{L}_{i-1}, P} \end{bmatrix} \quad (16)$$

Where:

$$\bullet \mathbf{L}_{kP} = \boldsymbol{\Phi}_{ik}^T \mathbf{M}_{fr} \quad \bullet \mathbf{c}_{kk} = \text{diag}(2\xi_k \omega_k) \quad \bullet \mathbf{k}_{kk} = \text{diag}(\omega_k^2)$$

The state space system can be directly obtained from this formulation, thanks to the relation:

$$\ddot{\mathbf{u}}_C = \boldsymbol{\Phi}_{Ck} \dot{\boldsymbol{\eta}}_k + \boldsymbol{\tau}_{CP} \ddot{\mathbf{u}}_P \quad (17)$$

The resulting system is therefore showcased in Eq. 18, where the state-space system  $\mathbf{D}_{PC}^{\mathcal{L}_i}(s)$  is the TITOP model corresponding to the one of Fig. 1.

$$\begin{bmatrix} \dot{\eta}_k \\ \ddot{\eta}_k \\ \ddot{\mathbf{u}}_C \\ \mathbf{W}_{\mathcal{L}_i/\mathcal{L}_{i-1},P} \end{bmatrix} = \underbrace{\begin{bmatrix} \mathbf{0}_{kk} & \mathbf{I}_{kk} & \mathbf{0}_{kC} & \mathbf{0}_{kP} \\ -\mathbf{k}_{kk} & -\mathbf{c}_{kk} & \Phi_{Ck}^T & -\mathbf{L}_{kP} \\ -\Phi_{Ck}\mathbf{k}_{kk} & -\Phi_{Ck}\mathbf{c}_{kk} & \Phi_{Ck}\Phi_{Ck}^T & (\boldsymbol{\tau}_{CP} - \Phi_{Ck}\mathbf{L}_{kP}) \\ \mathbf{L}_{kP}^T\mathbf{k}_{kk} & \mathbf{L}_{kP}^T\mathbf{c}_{kk} & (\boldsymbol{\tau}_{CP} - \Phi_{Ck}\mathbf{L}_{kP})^T & \mathbf{L}_{kP}^T\mathbf{L}_{kP} - \mathbf{M}_{rr} \end{bmatrix}}_{\mathbf{D}_{PC}^{\mathcal{L}_i}(s)} \begin{bmatrix} \eta_k \\ \dot{\eta}_k \\ \ddot{\mathbf{u}}_P \\ \mathbf{W}_{\mathcal{L}_{i+1}/\mathcal{L}_i,C} \end{bmatrix} \quad (18)$$

### 3 ANALYTICALLY INVERTED TITOP MODEL

#### 3.1 TITOP Beam Models and Closed-Loop Kinematics

The TITOP beam model detailed in section 2.2 presents a specific set of boundary conditions. Despite this, the importance of handling different boundary conditions plays a fundamental role in the correct modeling of complex systems, specifically in closed-loop kinematics.

For instance, let us consider a basic closed-loop mechanism, such as a triangle, which can be used as a building block to assembly more complex structures using a sub-structuring approach.

This mechanism, composed by three flexible bodies and represented in Fig. 2a, can be imagined clamped to a parent body  $\mathcal{L}_0$  at point A and being submitted to efforts coming from two external bodies  $\mathcal{L}_4$  and  $\mathcal{L}_5$  attached at points B and C respectively.

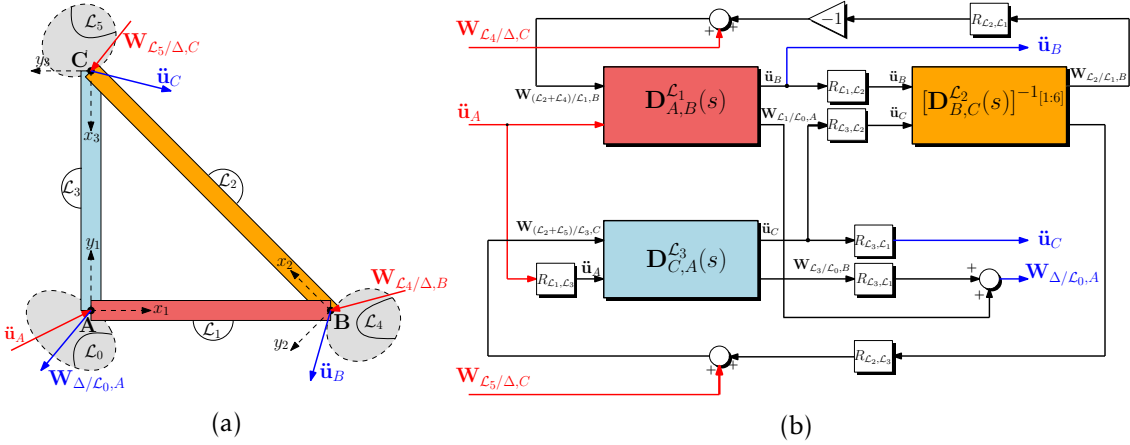


**Figure 2.** Block diagram of the  $\Delta$  mechanism, showcased in 2a and modeled in 2b in the TITOP framework. Note that the blocks  $R_{i,j}$  represent the rotation matrices between the  $i$ -th and  $j$ -th frames of references.

The triangular structure, which can be denoted as  $\Delta$ , can be modeled as a dynamic system whose inputs are the accelerations  $\ddot{\mathbf{u}}_A$  imposed at point A by  $\mathcal{L}_0$  and the external efforts  $\mathbf{W}_{\mathcal{L}_4/\Delta,B}$ ,  $\mathbf{W}_{\mathcal{L}_5/\Delta,C}$  applied by the bodies  $\mathcal{L}_4$  and  $\mathcal{L}_5$  to the triangle mechanism  $\Delta$ .

In the context of a sub-structuring approach, the triangular structure  $\Delta$  can be conceived as an assembly of multiple TITOP models, as seen in Fig. 2b. These blocks have to be properly connected in order to impose the correct input-output configuration and to close the kinematic loop.

The only way to achieve this result is to use not only *clamped-free* models, but a *clamped-clamped* TITOP model as well. In fact, at sub-structure level, the two beams  $\mathcal{L}_1$  and  $\mathcal{L}_3$

can be considered *clamped-free* using the two direct TITOP models  $\mathbf{D}_{A,B}^{\mathcal{L}_1}(s)$  and  $\mathbf{D}_{A,C}^{\mathcal{L}_3}(s)$ , as they have an acceleration imposed by a parent body at point  $A$  and are submitted to an effort by external bodies at points  $B$  and  $C$ . The assembly of the closed-loop is then achieved by imposing force/moment balance at each node of the structure. Since the distribution of the external efforts on the different beams is unknown, the third beam  $\mathcal{L}_2$  is considered with accelerations imposed at both ends: the accelerations outputted by the TITOP models of  $\mathcal{L}_1$  and  $\mathcal{L}_3$  are the inputs of the TITOP block of  $\mathcal{L}_2$ , as this allows for the retrieval of the reaction forces exerted by  $\mathcal{L}_2$  to the other bodies, namely  $\mathbf{W}_{\mathcal{L}_2/\mathcal{L}_1,B}$  and  $\mathbf{W}_{\mathcal{L}_2/\mathcal{L}_3,C}$ . This means considering a TITOP model with the first six channels inverted,  $[\mathbf{D}_{B,C}^{\mathcal{L}_2}(s)]^{-1(1:6)}$ , that represents a *clamped-clamped* beam.

A numerical procedure to invert the channels of a TITOP model has been introduced in [5]. The following section provides a new analytical formulation for the *clamped-clamped* beam that solves the numerical issues found in the current TITOP model channel inversion.

### 3.2 Mathematical Formulation

An analytical inversion is here proposed for the first six channels of the original TITOP beam model introduced in section 2.2, which correspond to the free node  $C$ .

The inversion process aims at obtaining the analytically inversed model  $[\mathbf{D}_{PC}^A(s)]_{ana}^{-1(1:6)}$  whose input-output configuration reflects a *clamped-clamped* boundary condition applied to the beam. As depicted in Fig. 3, the inputs of the system are the endpoint accelerations  $\ddot{\mathbf{u}}_P$  and  $\ddot{\mathbf{u}}_C$ , while the corresponding outputs are the efforts on those points, which are still maintaining the same formalism of the original TITOP model.

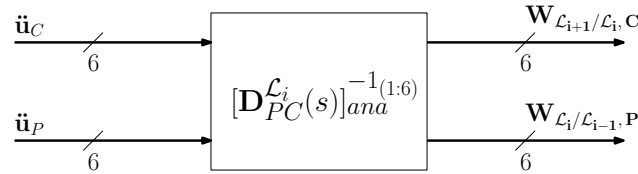


**Figure 3.** Input-output configuration for the analytically inverted *clamped-clamped* TITOP beam model

A change of variables is applied to the system in Eq. 16. We introduce vector  $\boldsymbol{\epsilon}_k$ , partitioned in two sub-vectors:  $\boldsymbol{\epsilon}_{k_1}$  and  $\boldsymbol{\epsilon}_{k_2}$ . The first one, of size  $\{6 \times 1\}$ , corresponds to the twelve poles at exactly zero frequency of the system. This is done to enforce the *clamped-clamped* boundary condition. The second vector, on the other hand, has a size of  $\{4 \times 1\}$  and determines the internal vibrational response of the system. The modal coordinates can be rewritten as:

$$\boldsymbol{\eta}_k = \mathbf{F}\boldsymbol{\epsilon}_k = \begin{bmatrix} \boldsymbol{\Phi}_{Ck}^+ & null(\boldsymbol{\Phi}_{Ck}) \end{bmatrix} \begin{bmatrix} \boldsymbol{\epsilon}_{k_1} \\ \boldsymbol{\epsilon}_{k_2} \end{bmatrix} \quad (19)$$

where the  $(\cdot)^+$  operator denotes the generalized inverse (or pseudo-inverse) of the non-square matrix and  $null(\cdot)$  the null space operator (or kernel). The use of this last operator allows the creation of a model whose modes corresponding to  $\boldsymbol{\epsilon}_{k_1}$  are intrinsically set to zero, while the modes associated to  $\boldsymbol{\epsilon}_{k_2}$  do not get simplified.

The first state equation for the new system can be directly derived from Eq. 19. By substituting this equation into Eq. 17, an explicit expression for  $\boldsymbol{\epsilon}_{k_1}$  may be obtained as

function of the two inputs  $\ddot{\mathbf{u}}_P$  and  $\ddot{\mathbf{u}}_C$ .

$$\ddot{\boldsymbol{\epsilon}}_{k_1} = \boldsymbol{\Phi}_{Ck} \mathbf{F} \ddot{\boldsymbol{\epsilon}}_k = \begin{bmatrix} \mathbf{I} & \mathbf{0} \end{bmatrix} \ddot{\boldsymbol{\epsilon}}_k = \ddot{\mathbf{u}}_C - \boldsymbol{\tau}_{CP} \ddot{\mathbf{u}}_P \quad (20)$$

The change of variables may be performed on the modal equations of motion in Eq. 18:

$$\ddot{\boldsymbol{\epsilon}}_k = \begin{bmatrix} \ddot{\boldsymbol{\epsilon}}_{k_1} & \ddot{\boldsymbol{\epsilon}}_{k_2} \end{bmatrix}^T = -\bar{\mathbf{k}}_{kk} \boldsymbol{\epsilon}_k - \bar{\mathbf{c}}_{kk} \dot{\boldsymbol{\epsilon}}_k - \mathbf{F}^{-1} \mathbf{L}_{kP} \ddot{\mathbf{u}}_P + \mathbf{F}^{-1} \boldsymbol{\Phi}_{Ck}^T \mathbf{W}_{\mathcal{L}_{i+1}/\mathcal{L}_i, C} \quad (21)$$

where  $\bar{\mathbf{k}}_{kk} = \mathbf{F}^{-1} \mathbf{k}_{kk} \mathbf{F}$  and  $\bar{\mathbf{c}}_{kk} = \mathbf{F}^{-1} \mathbf{c}_{kk} \mathbf{F}$ . Moreover, this expression may be rewritten in order to explicit the two sub-vectors which compose vector  $\boldsymbol{\epsilon}_k$ , therefore obtaining a set of two equations. The following notation is hereby introduced, which defines the partition of matrices  $\bar{\mathbf{k}}_{kk}$  and  $\bar{\mathbf{c}}_{kk}$ :  $\bar{\mathbf{X}} = \begin{bmatrix} \bar{\mathbf{X}}_{11} & \bar{\mathbf{X}}_{12} \\ \bar{\mathbf{X}}_{21} & \bar{\mathbf{X}}_{22} \end{bmatrix}$ .

The first of the two equations obtained from Eq. 21, expressing  $\ddot{\boldsymbol{\epsilon}}_{k_1}$ , is:

$$\ddot{\boldsymbol{\epsilon}}_{k_1} = -\bar{\mathbf{k}}_{kk_{11}} \boldsymbol{\epsilon}_{k_1} - \bar{\mathbf{k}}_{kk_{12}} \boldsymbol{\epsilon}_{k_2} - \bar{\mathbf{c}}_{kk_{11}} \dot{\boldsymbol{\epsilon}}_{k_1} - \bar{\mathbf{c}}_{kk_{12}} \dot{\boldsymbol{\epsilon}}_{k_2} + \boldsymbol{\Phi}_{Ck} \boldsymbol{\Phi}_{Ck}^T \mathbf{W}_{\mathcal{L}_{i+1}/\mathcal{L}_i, C} - \boldsymbol{\Phi}_{Ck} \mathbf{L}_{kP} \ddot{\mathbf{u}}_P \quad (22)$$

An explicit expression for  $\mathbf{W}_{\mathcal{L}_{i+1}/\mathcal{L}_i, C}$  can be derived from this equation, substituting  $\ddot{\boldsymbol{\epsilon}}_{k_1}$  by inverting Eq. 20. This represents the first output equation for the new state-space system:

$$\begin{aligned} \mathbf{W}_{\mathcal{L}_{i+1}/\mathcal{L}_i, C} = (\boldsymbol{\Phi}_{Ck}^T)^+ \boldsymbol{\Phi}_{Ck}^+ & \left( \bar{\mathbf{k}}_{kk_{11}} \boldsymbol{\epsilon}_{k_1} + \bar{\mathbf{k}}_{kk_{12}} \boldsymbol{\epsilon}_{k_2} + \bar{\mathbf{c}}_{kk_{11}} \dot{\boldsymbol{\epsilon}}_{k_1} \right. \\ & \left. + \bar{\mathbf{c}}_{kk_{12}} \dot{\boldsymbol{\epsilon}}_{k_2} + \ddot{\mathbf{u}}_C + (\boldsymbol{\Phi}_{Ck} \mathbf{L}_{kP} - \boldsymbol{\tau}_{CP}) \ddot{\mathbf{u}}_P \right) \end{aligned} \quad (23)$$

which can be rewritten in the form:

$$\mathbf{W}_{\mathcal{L}_{i+1}/\mathcal{L}_i, C} = \mathbf{C}_{11} \boldsymbol{\epsilon}_{k_1} + \mathbf{C}_{12} \boldsymbol{\epsilon}_{k_2} + \mathbf{C}_{13} \dot{\boldsymbol{\epsilon}}_{k_1} + \mathbf{C}_{14} \dot{\boldsymbol{\epsilon}}_{k_2} + \mathbf{D}_{11} \ddot{\mathbf{u}}_C + \mathbf{D}_{12} \ddot{\mathbf{u}}_P \quad (24)$$

Where:

- $\mathbf{C}_{11} = (\boldsymbol{\Phi}_{Ck}^T)^+ \boldsymbol{\Phi}_{Ck}^+ \bar{\mathbf{k}}_{kk_{11}}$ ;
- $\mathbf{C}_{12} = (\boldsymbol{\Phi}_{Ck}^T)^+ \boldsymbol{\Phi}_{Ck}^+ \bar{\mathbf{k}}_{kk_{12}}$ ;
- $\mathbf{C}_{13} = (\boldsymbol{\Phi}_{Ck}^T)^+ \boldsymbol{\Phi}_{Ck}^+ \bar{\mathbf{c}}_{kk_{11}}$ ;
- $\mathbf{C}_{14} = (\boldsymbol{\Phi}_{Ck}^T)^+ \boldsymbol{\Phi}_{Ck}^+ \bar{\mathbf{c}}_{kk_{12}}$ ;
- $\mathbf{D}_{11} = (\boldsymbol{\Phi}_{Ck}^T)^+ \boldsymbol{\Phi}_{Ck}^+$ ;
- $\mathbf{D}_{12} = (\boldsymbol{\Phi}_{Ck}^T)^+ \boldsymbol{\Phi}_{Ck}^+ (\boldsymbol{\Phi}_{Ck} \mathbf{L}_{kP} - \boldsymbol{\tau}_{CP})$

The second equation in Eq. 21 describes the behavior of  $\ddot{\boldsymbol{\epsilon}}_{k_2}$ :

$$\begin{aligned} \ddot{\boldsymbol{\epsilon}}_{k_2} = -\bar{\mathbf{k}}_{kk_{21}} \boldsymbol{\epsilon}_{k_1} - \bar{\mathbf{k}}_{kk_{22}} \boldsymbol{\epsilon}_{k_2} - \bar{\mathbf{c}}_{kk_{21}} \dot{\boldsymbol{\epsilon}}_{k_1} - \bar{\mathbf{c}}_{kk_{22}} \dot{\boldsymbol{\epsilon}}_{k_2} \\ - \text{null}(\boldsymbol{\Phi}_{Ck})^T \boldsymbol{\Phi}_{Ck}^T \mathbf{W}_{\mathcal{L}_{i+1}/\mathcal{L}_i, C} - \text{null}(\boldsymbol{\Phi}_{Ck})^T \mathbf{L}_{kP} \ddot{\mathbf{u}}_P \end{aligned} \quad (25)$$

Note that by definition of the kernel operator,  $\boldsymbol{\Phi}_{Ck} \cdot \text{null}(\boldsymbol{\Phi}_{Ck}) = \mathbf{0}$ . Therefore also  $\text{null}(\boldsymbol{\Phi}_{Ck})^T \boldsymbol{\Phi}_{Ck}^T = \mathbf{0}$ . This property has the effect of canceling the contribution of

**Table 1.** Parameters of TITOP Beams used for the case study

$l[m]$	$S[m^2]$	$\rho[kg/m^2]$	$E[GPa]$	$\nu$	$I_y[m^{-4}]$	$I_z[m^{-4}]$	$\xi$
20	0.0004	2700	70	0.35	6.7e-7	6.7e-7	0.001

$\mathbf{W}_{\mathcal{L}_{i+1}/\mathcal{L}_i,C}$  to the second order dynamics of  $\boldsymbol{\epsilon}_{k_2}$ , allowing for an explicit expression of  $\ddot{\boldsymbol{\epsilon}}_{k_2}$  as function of state variables and inputs only.

The final expression needed to complete the TITOP model is the output equation for  $\mathbf{W}_{\mathcal{L}_i/\mathcal{L}_{i-1},P}$ . This can be easily obtained from the outputs of Eq. 18, to which the change of state variables is applied. The resulting equation is:

$$\mathbf{W}_{\mathcal{L}_i/\mathcal{L}_{i-1},P} = \mathbf{C}_{21}\boldsymbol{\epsilon}_{k_1} + \mathbf{C}_{22}\dot{\boldsymbol{\epsilon}}_{k_1} + \mathbf{C}_{23}\boldsymbol{\epsilon}_{k_2} + \mathbf{C}_{24}\dot{\boldsymbol{\epsilon}}_{k_2} + \mathbf{D}_{21}\ddot{\mathbf{u}}_C + \mathbf{D}_{22}\ddot{\mathbf{u}}_P \quad (26)$$

Where:

- $\mathbf{LKF} = \mathbf{L}_{kP}^T \mathbf{k}_{kk} \mathbf{F}$ ;
- $\mathbf{LCF} = \mathbf{L}_{kP}^T \mathbf{c}_{kk} \mathbf{F}$ ;
- $\mathbf{TPL} = (\boldsymbol{\tau}_{CP} - \boldsymbol{\Phi}_{Ck} \mathbf{L}_{kP})$ ;
- $\mathbf{C}_{21} = \mathbf{LKF}(:, 1:6) + \mathbf{TPL}^T (\boldsymbol{\Phi}_{Ck}^T)^+ \boldsymbol{\Phi}_{Ck}^+ \bar{\mathbf{k}}_{kk_{k1}}$ ;
- $\mathbf{C}_{22} = \mathbf{LKF}(:, 1:6) + \mathbf{TPL}^T (\boldsymbol{\Phi}_{Ck}^T)^+ \boldsymbol{\Phi}_{Ck}^+ \bar{\mathbf{c}}_{kk_{k1}}$ ;
- $\mathbf{C}_{23} = \mathbf{LKF}(:, 7:10) + \mathbf{TPL}^T (\boldsymbol{\Phi}_{Ck}^T)^+ \boldsymbol{\Phi}_{Ck}^+ \bar{\mathbf{k}}_{kk_{k2}}$ ;
- $\mathbf{C}_{24} = \mathbf{LKF}(:, 7:10) + \mathbf{TPL}^T (\boldsymbol{\Phi}_{Ck}^T)^+ \boldsymbol{\Phi}_{Ck}^+ \bar{\mathbf{c}}_{kk_{k2}}$ ;
- $\mathbf{D}_{22} = \mathbf{TPL}^T (\boldsymbol{\Phi}_{Ck}^T)^+ \boldsymbol{\Phi}_{Ck}^+$ ;
- $\mathbf{D}_{22} = \mathbf{L}_{kP}^T \mathbf{L}_{kP} - \mathbf{M}_{rr} + \mathbf{TPL}^T (\boldsymbol{\Phi}_{Ck}^T)^+ \boldsymbol{\Phi}_{Ck}^+ \mathbf{TPL}$

These results can be used to obtain a TITOP Model for the inversed *clamped-clamped* beam. By using the results of Eq.s 20,24,25,26, the final system can be assembled as follows

$$\begin{bmatrix} \dot{\boldsymbol{\epsilon}}_{k_1} \\ \ddot{\boldsymbol{\epsilon}}_{k_1} \\ \dot{\boldsymbol{\epsilon}}_{k_2} \\ \ddot{\boldsymbol{\epsilon}}_{k_2} \\ \mathbf{W}_{\mathcal{L}_{i+1}/\mathcal{L}_i,C} \\ \mathbf{W}_{\mathcal{L}_i/\mathcal{L}_{i-1},P} \end{bmatrix} = \underbrace{\begin{bmatrix} \mathbf{0}_{k_1 k_1} & \mathbf{I}_{k_1 k_1} & \mathbf{0}_{k_1 k_2} & \mathbf{0}_{k_1 k_2} & \mathbf{0}_{k_1 C} & \mathbf{0}_{k_1 P} \\ \mathbf{0}_{k_1 k_1} & \mathbf{0}_{k_1 k_1} & \mathbf{0}_{k_1 k_2} & \mathbf{0}_{k_1 k_2} & \mathbf{I}_{k_1 C} & -\boldsymbol{\tau}_{CP} \\ \mathbf{0}_{k_2 k_1} & \mathbf{0}_{k_2 k_1} & \mathbf{0}_{k_2 k_2} & \mathbf{I}_{k_2 k_2} & \mathbf{0}_{k_2 C} & \mathbf{0}_{k_2 P} \\ -\bar{\mathbf{k}}_{kk_{k2}} & -\bar{\mathbf{c}}_{kk_{k1}} & -\bar{\mathbf{k}}_{kk_{k2}} & -\bar{\mathbf{c}}_{kk_{k2}} & \mathbf{0}_{k_2 C} & -null(\boldsymbol{\Phi}_{Ck})^T \mathbf{L}_{kP} \\ \mathbf{C}_{11} & \mathbf{C}_{12} & \mathbf{C}_{13} & \mathbf{C}_{14} & \mathbf{D}_{11} & \mathbf{D}_{12} \\ \mathbf{C}_{21} & \mathbf{C}_{22} & \mathbf{C}_{23} & \mathbf{C}_{24} & \mathbf{D}_{21} & \mathbf{D}_{22} \end{bmatrix}}_{\left[ \mathbf{D}_{PC}^{\mathcal{L}_i}(s) \right]_{ana}^{-1[1:6]}} \begin{bmatrix} \boldsymbol{\epsilon}_{k_1} \\ \dot{\boldsymbol{\epsilon}}_{k_1} \\ \boldsymbol{\epsilon}_{k_2} \\ \dot{\boldsymbol{\epsilon}}_{k_2} \\ \ddot{\mathbf{u}}_C \\ \ddot{\mathbf{u}}_P \end{bmatrix} \quad (27)$$

The  $\left[ \mathbf{D}_{PC}^{\mathcal{L}_i}(s) \right]_{ana}^{-1[1:6]}$  model in Eq. 27 is the analytically inversed *clamped-clamped* TITOP model showcased in Fig. 3.

#### 4 MODEL APPLICATION AND VALIDATION

In order to validate the accuracy of the newly derived model, the system has been verified by comparison to a reference theoretical beam model [3] as well as the numerically inverted TITOP beam of [5].

Given a homogeneous beam of length  $l$ , section  $S$ , density  $\rho$ , Young modulus  $E$ , Poisson's ratio  $\nu$ , second moments of inertia  $I_y, I_z$  along  $y$  and  $z$  axes and damping coefficient  $\xi$ , the parameters presented in Table 1 were used to obtain the singular value plots seen in Fig.4.

This plot describes the transfers between  $\ddot{\mathbf{u}}_P$  and  $\mathbf{W}_{\mathcal{L}_i/\mathcal{L}_{i-1},P}$  for both analytically and numerically inverted models. In particular we define:

$$\mathbf{G}_{\mathbf{W}_P, \ddot{\mathbf{u}}_P}^{ana}(s) = \left( \left[ \mathbf{D}_{PC}^{\mathcal{L}_i}(s) \right]_{ana}^{-1[1:6]} \right)_{\ddot{\mathbf{u}}_P \rightarrow \mathbf{W}_P}, \quad \mathbf{G}_{\mathbf{W}_P, \ddot{\mathbf{u}}_P}^{num}(s) = \left( \left[ \mathbf{D}_{PC}^{\mathcal{L}_i}(s) \right]_{num}^{-1[1:6]} \right)_{\ddot{\mathbf{u}}_P \rightarrow \mathbf{W}_P} \quad (28)$$

as the multiple-input-multiple-output transfers between  $\ddot{\mathbf{u}}_P$  and  $\mathbf{W}_{\mathcal{L}_i/\mathcal{L}_{i-1},P}$  for the analytically inverted  $\left[ \mathbf{D}_{PC}^{\mathcal{L}_i}(s) \right]_{ana}^{-1[1:6]}$  and the numerically inverted  $\left[ \mathbf{D}_{PC}^{\mathcal{L}_i}(s) \right]_{num}^{-1[1:6]}$  models.

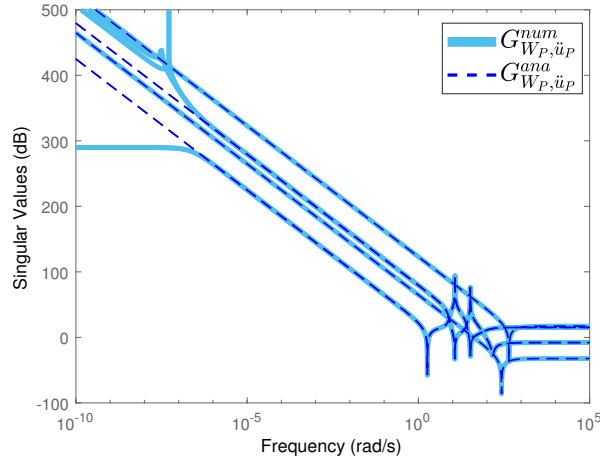


**Figure 4.** Singular values for the analytically  $\mathbf{G}_{\mathbf{W}_P, \ddot{\mathbf{u}}_P}^{ana}(s)$  and numerically  $\mathbf{G}_{\mathbf{W}_P, \ddot{\mathbf{u}}_P}^{num}(s)$  inverted TITOP models

The two responses match exactly except for near-to-zero frequency values: in this range the numerical inversion produces artificial behaviors like non-physical zeros and poles. The proposed analytical system overcomes these issues, granting an infinite gain at zero frequency with a correct  $1/s^2$  dynamics at low frequency. This is in fact the expected behavior of the system, where the imposition of non-compatible accelerations at the two extremities of the rigid beam produces infinite efforts.

These results are furthermore corroborated by comparing the modes of the two models: Table 2 shows the normalized natural frequencies of the two *clamped-clamped* models - analytical and numerical. The frequencies, normalized by  $\sqrt{\frac{EI}{\rho SI^4}}$ , are also compared to the reference theoretical values expected for each mode.

A study of Table 2 shows how the introduction of the analytical model solved the non-zero poles issues found in the numerically inverted TITOP model, while granting the same level of accuracy in the description of the vibrational phenomena. The last four

**Table 2.** Comparison of the natural frequencies, normalized by  $\sqrt{\frac{EI}{\rho SI^4}}$ , of the numerically inverted TITOP model ( $\omega_{k,num}$ ) and the new analytically inverted model ( $\omega_{k,ana}$ ) to the reference theoretical value  $\omega_{ref}$

<i>Mode k</i>	$\omega_{k,ref}$	$\omega_{k,num}$	$\omega_{k,ana}$	<i>Mode k</i>	$\omega_{k,ref}$	$\omega_{k,num}$	$\omega_{k,ana}$
1	0	0.00	0.00	6	0	9.15e-08	0.00
2	0	0.00	0.00	7	22.373	22.450	22.450
3	0	6.04e-17	0.00	8	22.373	22.450	22.450
4	0	2.28e-14	0.00	9	61.673	62.929	62.929
5	0	9.15e-08	0.00	10	61.673	62.929	62.929

flexible modes are in fact corresponding exactly to the modes found in [5] for the bending of a *clamped-clamped* beam, and represent a good approximation of the reference frequency value.

## 5 CONCLUSIONS

An analytical model of a *clamped-clamped* TITOP beam was derived in order to overcome the limits of the numerical inversion of the *clamped-free* TITOP model.

The proposed model has been validated by theoretical results and it represents a building block for modeling more complex multi-body flexible structures in closed-loop configurations.

## REFERENCES

- [1] Theodore, R.J., Ghosal, A.: Comparison of the assumed modes and finite element models for flexible multilink manipulators. *The International Journal of Robotics Research* **14**(2) (1995) 91–111
- [2] Leckie, F., Pestel, E.: Transfer-matrix fundamentals. *International Journal of Mechanical Sciences* **2**(3) (1960) 137 – 167
- [3] Girard, A., Roy, N.: *Structural Dynamics in Industry*. Wiley (2008)
- [4] Alazard, D., Perez, J.A., Cumer, C., Loquen, T.: Two-input two-output port model for mechanical systems. In: *AIAA Guidance, Navigation, and Control Conference*. (2015) 1778
- [5] Chebbi, J., Dubanchet, V., Perez Gonzalez, J.A.: Linear dynamics of flexible multi-body systems: A system-based approach. *Multibody System Dynamics* **41** (11 2016)
- [6] Alazard, D., Cumer, C.: *Satellite Dynamics Toolbox*. (2014)
- [7] Sanfedino, F., Alazard, D., Pommier-Budinger, V., Falcoz, A., Boquet, F.: Finite element based n-port model for preliminary design of multibody systems. *Journal of Sound and Vibration* **415** (2018) 128 – 146